

ARTICLE

Analysis of Turbulence on Cylinder with Additional Fairing with Free Surface

Siqin Chen¹ Xiaomin Li^{2*}

1.China University of Petroleum, Beijing, China

2.Yunnan Normal University College of Arts and Sciences, Kunming, China

ARTICLE INFO

Article history

Received: 1 December 2020

Accepted: 27 January 2021

Published Online: 9 April 2021

Keywords:

Numerical simulation

Computational fluid dynamics (CFD)

Volume of fluid

Free surface of liquid

ABSTRACT

In this study, two dimensional unsteady flows of cylinder and cylinder with additional fairing close to a free surface were numerically investigated. The governing momentum equations were solved by using the Semi Implicit Method for Pressure Linked Equations(SIMPLE). The Volume of Fluid(VOF) method applied to simulate a free surface. Non- uniform grid structures were used in the simulation with denser grids near the cylinder. Under the conditions of Reynolds number 150624, 271123, 210874 and 331373, the cylinders were simulated with different depths of invasion. It was shown that the flow characteristics were influenced by submergence depth and Reynolds numbers. When the cylinder close to the free surface, the drag coefficient, lift coefficient and Strouhal numbers will increase due to the effect of free liquid surface on vortex shedding. With additional fairing, can effectively reduce the influence of the free surface on the drag coefficient. Fairing will reduce lift coefficient at high Reynolds numbers, but increase lift coefficient when Reynolds numbers are small. Fairing can effectively reduce Strouhal numbers, thus can well suppress the vortex induced vibration.

1. Introduction

In many ocean engineering, shipbuilding engineering, etc., the phenomenon of fluid pressure and atmosphere communication is widespread. In actual engineering, deep-sea drilling, underwater oil and gas pipelines will all affect the surrounding flow field under the action of free liquid surface. Due to the effect of wind load in the entire field, the phenomenon of air inhalation and bubble collapse of the cylinder in the flow field, the study of the hydrodynamic characteristics of the free surface structure has become one of the research problems. Among them, the flow around a cylinder is one of the classic problems

in hydrodynamics.

Researchers have achieved effective results on the problem of flow around a cylinder that ignores the phenomenon of free surface motion under the condition of low Reynolds number, and the related problems of high Reynolds number are still being discussed and studied. In 1961, A. Roshko^[1] conducted a flow experiment around a cylinder under a high Reynolds number ($10^6 < Re < 10^7$) in a wind tunnel, and found that when $Re > 3.5 \times 10^6$, the drag coefficient tends to a constant 0.7 and St is stable at 0.27. In 1964, Hseh obtained the relationship curve of the total resistance coefficient with the Fr number, that is, the resistance value reached the maximum when Fr was approxi-

*Corresponding Author:

Xiaomin Li,

Yunnan Normal University College of Arts and Sciences, Kunming, China;

Email: 2562275375@qq.com

mately equal to 1. In 1969, Bearman [2] conducted experiments on the vortex shedding phenomenon with Reynolds number in the range of $2 \times 10^5 < Re < 5.5 \times 10^5$ in the circulating water tank, and measured the resistance, pulsating lift, St and other hydrodynamic parameters under different Reynolds numbers. In 1983, G. Schewe [3] conducted a wind tunnel experiment on the flow around a cylinder in the range of $2.3 \times 10^4 < Re < 7.1 \times 10^6$ for the Reynolds number, and obtained a steep drop in the drag coefficient and an increase in the Steroha number and other changes.

In 2003, Chaplin and Teigen found that the local resistance near the free surface is reduced. Yu [4], Suh [5], Graf [6], Kawamura [7] and others have carried out related numerical simulation studies, and also proved that when the Re number is less than 1.4×10^5 , the drag coefficient at the liquid surface is less than 1.2.

In 2004, Chui-Jie Wu [8] used the dynamic boundary control technology to study the flow around a cylinder and found that the moving wave wall can effectively suppress the separation of the flow vortex around the cylinder and eliminate the oscillation wake. In 2005, Choi [9] found that the distribution of sinusoidal pressure with a specific phase angle in the span direction can significantly reduce the fluctuation of average drag and lift. In 2013, Wu Yucheng [10] studied the influence of the fairing on the flow field. Experimental results show that the fairing can improve the flow field and reduce the fluid resistance of the structure by more than 50%.

In the current research, most of the analysis of flow around a cylinder does not consider the influence of free liquid on its flow. In some pools, due to the small depth of the pool, the pipeline will be closer to the water surface. In this case, the influence of the free surface needs to be considered when analyzing the surrounding flow field. The main purpose of this article is to study the effect of free surface on vortex-Induced vibration and how to eliminate these effects.

2. Numerical Theory

2.1 Governing Equations

The basic governing equations of fluid dynamics include continuity equation, momentum equation and energy conservation equation. In this paper, considering water medium as an incompressible fluid, while air medium had less effect on the results, and it can also be simplified as an ideal gas. Continuity equation and momentum conservation equation should be considered when setting parameters. Continuity equation and momentum conservation equation are given in Equation (1) and Equation (2).

$$\nabla \cdot \mathbf{u} = 0 \tag{1}$$

$$\frac{\partial}{\partial t}(\rho \mathbf{u}) + \nabla \cdot (\rho \mathbf{u} \otimes \mathbf{u}) = \nabla \cdot (\mu \nabla \otimes \mathbf{u}) - \nabla P + \rho \mathbf{g} \tag{2}$$

\mathbf{u} , ρ , P and \mathbf{g} represent the velocity vector, fluid density, pressure and gravitational acceleration.

2.2 Turbulence Model

k - ε model with two equations is the most widely used model for viscous flow. This model is further divided into standard k - ε model, RNG k - ε model and Realizable k - ε model.

Standard k - ε model assuming that the flow is completely turbulent, the influence of molecular viscosity can be ignored. The model has a wide range of applications and reasonable accuracy, and it is the main tool in engineering flow field calculations. It's formed by new equation of turbulence dissipation rate on the basis of the original single equation model. This model requires the flow field is assumed to be complete turbulence field. In this study, standard k - ε model was chosen. Turbulent kinetic energy equation and turbulent dissipation equation are given in Equation (2) and Equation (3).

$$\frac{\partial(\rho k)}{\partial t} + \frac{\partial(\rho k u_i)}{\partial x_i} = \frac{\partial}{\partial x_j} \left[\left(\mu + \frac{\mu_t}{\sigma_k} \right) \frac{\partial k}{\partial x_j} \right] + G_k + G_b - \rho \varepsilon - Y_M + S_k \tag{3}$$

$$\frac{\partial(\rho \varepsilon)}{\partial t} + \frac{\partial(\rho \varepsilon u_i)}{\partial x_i} = \frac{\partial}{\partial x_j} \left[\left(\mu + \frac{\mu_t}{\sigma_\varepsilon} \right) \frac{\partial \varepsilon}{\partial x_j} \right] + C_{1\varepsilon} \frac{\varepsilon}{k} (G_k + C_{3\varepsilon} G_b) - C_{2\varepsilon} \rho \frac{\varepsilon^2}{k} + S_\varepsilon \tag{4}$$

G_k , G_b represent turbulent kinetic energy due to mean velocity gradient, turbulent kinetic energy due to buoyancy. σ_k and σ_ε represent the turbulence Prandtl number corresponding to k and ε , S_k and S_ε are defined by user, $C_{1\varepsilon}$, $C_{2\varepsilon}$ and $C_{3\varepsilon}$ are empirical constant.

2.3 Flow Parameters

Drag coefficient is a dimensionless number of the effect of momentum transfer to the ground. Lift coefficient is a dimensionless coefficient that relates the lift force generated by a lift to the density of the nearby fluid, the fluid velocity, and the associated reference area. Those are important parameters in fluid flow analysis.

Calculations of the drag and lift coefficients on the cylinder surfaces are given in Equation (5), (6). Drag and lift forces are calculated by the viscous and pressure forces on the surfaces of the cylinders. The formulas are given in

Equation (7), (8). The Strouhal number is given in Equation (9).

$$CL_{mean} = \frac{2F_L}{\rho U_\infty^2 D} \tag{5}$$

$$CD_{mean} = \frac{2F_D}{\rho U_\infty^2 D} \tag{6}$$

$$F_D = \int_0^D (\tau_t(x) + \tau_b(x)) dx + \int_0^D (P_{fr}(y) + P_\tau(y)) dy \tag{7}$$

$$F_L = \int_0^D (\tau_{fr}(y) + \tau_r(y)) dy + \int_0^D (P_t(x) + P_b(x)) dx \tag{8}$$

$$St = \frac{fD}{U_\infty} \tag{9}$$

In Equation (7), (8), fr, r, t and b represent the front, back, upper and lower surfaces of cylinders respectively, D represents characteristic length of the structure. In Equation (9), f represents the vortex shedding frequency.

2.4 Multiphase Flow Model

The multiphase flow model in fluent has three types: Volume of Fluid Model (VOF model), Mixture model and Euler model. Among them, the VOF model is suitable for dealing with multiphase flow problems that do not intersect each other, such as free surface flow problems. The Mixture model is suitable for the flow analysis of particles in fluids including low powder-carrying airflow and bubble-containing flow. Euler model is suitable for bubble column, casting riser, particle suspension and other problems. In this case, it is more appropriate to choose the VOF model due to the study of free surface flow.

2.4.1 Continuity Equation

Tracking the interface between the phases is accomplished by solving the continuous equation of the volume ratio of one or more phases. For the qth phase, there is:

$$\frac{\partial \alpha_q}{t} + \vec{v} \cdot \alpha_q = \frac{S_{aq}}{\rho_q} \tag{10}$$

Among them: S_{aq} is the mass source term. By default, the source term at the right end of Equation (10) is zero, but when you specify a constant or user-defined mass

source for each phase, the right end is not zero. The calculation of the volume fraction of the main phase is based on the following constraints:

$$\sum_{q=1}^n \alpha_q = 1 \tag{11}$$

2.4.2 Attribute Calculation

The attributes that appear in the transport equation are determined by the phases that exist in each control volume. Assuming that in a two-phase flow system, the phases are represented by subscripts 1 and 2. If the volume fraction of the second phase is tracked, the density in each unit is as follows:

$$\rho = \alpha_2 \rho_2 + (1 - \alpha_2) \rho_1 \tag{12}$$

Generally, for an n-phase system, the volume ratio average density takes the following form:

$$\rho = \sum \alpha_q \rho_q \tag{13}$$

2.4.3 Momentum Equation

By solving a single momentum equation in the entire region, the velocity field obtained is shared by each phase. The momentum equation depends on the volume ratio of all phases passing through the properties ρ and μ , and the equation is as follows:

$$\frac{\partial}{\partial t} (\rho \vec{v}) + \nabla \cdot (\rho \vec{v} \vec{v}) = -\nabla p + [\mu (\nabla \vec{v} + \nabla \vec{v}^T)] + p \vec{g} + \vec{F} \tag{14}$$

2.4.4 Energy Equation

The energy equation is also shared in each phase, expressed as follows:

$$\frac{\partial}{\partial t} (\rho E) + \nabla \cdot [\vec{v} (\rho E + p)] = \nabla \cdot (k_{eff} \nabla T) + S_h \tag{15}$$

In this equation, k_{eff} is effective thermal conductivity, S_h is source terms, including radiation and other volumetric heat sources, E is total energy.

2.5 Numerical Details

In order to compare the results with actual test results, the parameters we choose in this study all refer to the parameters used in the actual test.

The cylinder and the computational domain are shown

in Figure 1, and 2D model was used in this simulation. The diameter of the cylinder(D) was 0.3048m; the distance between free surface and the center of the cylinder(H) was 1D; 2D; 3D; 4D and 5.5D. Cylinder with additional fairing and the computational domain are shown in Figure 2, expect for changing the structure. Other conditions are all same as the cylinder model does.

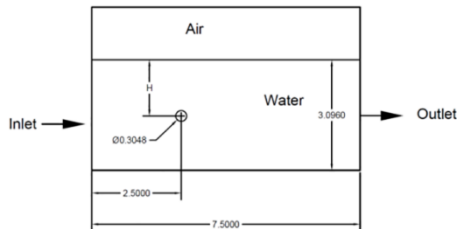


Figure 1. Computational domain for cylinder close to a free surface

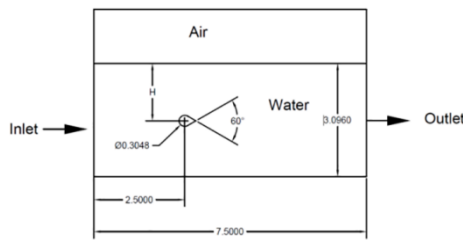


Figure 2. Computational domain for cylinder with additional fairing close to a free surface

A non-uniform grid structure was used, grids around the cylinder and the fairing are presented in Figure 3 and Figure 4.

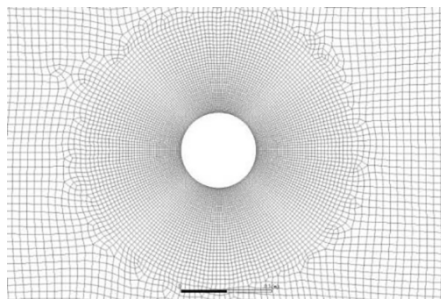


Figure 3. Grid around the cylinder

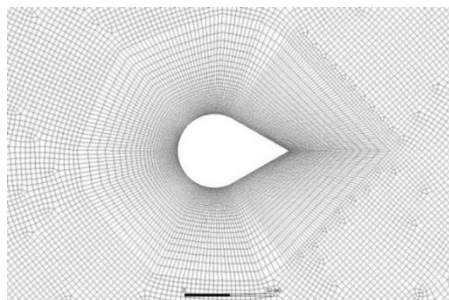


Figure 4. Grid around the cylinder with addition fairing

Simulations were performed at the Reynolds numbers(Re) 150624, 210874, 271123, 331373. Inlet was set as velocity inlet, outlet was set as outflow, all boundaries about air were set as symmetry, the structure and the lower boundary were set as wall. Multiphase model chose VOF model and viscous model chose standard $k-\epsilon$ model. SIMPLE algorithm is adopted for pressure velocity coupling, Least-Squares Cell Based interpolation algorithm was adopted, transient format was adopted Second order Implicit, pressure difference algorithm was adopted second order format, and momentum difference algorithm was adopted Second order format. All residual accuracy controls were set as 10^{-4} .

Choose the Cd value comparison under the Reynolds number 210874, H/D=5 to check the grid independence, and the results are as follows:

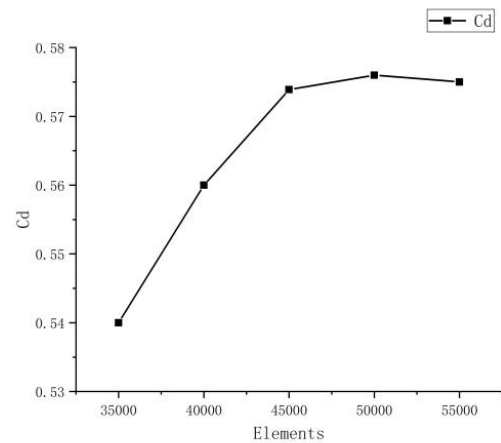


Figure 5(a). The grid dependency tests for cylinder

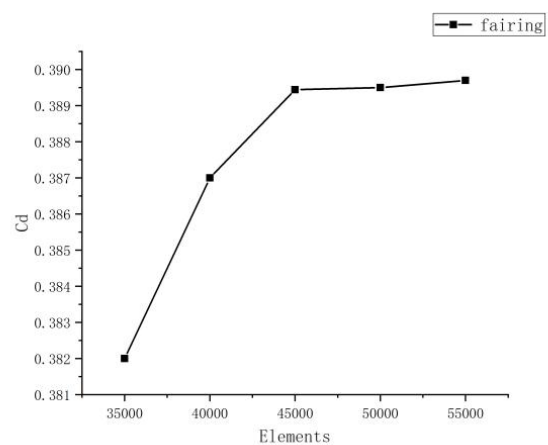


Figure 5(b). The grid dependency tests for fairing

According to the results of the grid independence check, 45,000 elements and 46,000 nodes are selected for simulation

3. Results and Discussions

2.1 Results of Cylinder

3.1.1 Effect of Submergence Depth

Figure 6 presents the vorticity magnitude at various submergence depth for $Re=331373$, when $H \geq 2D$, the more cylinder close to the free surface, the more vortex shedding becomes intense. On the one hand, because of the influence of free surface, some vortices fall off before they develop into larger size vortices. When $H=1D$, free surface will affect the formation of vortices, as Figure 6(e) presenting, there are no vortices formed under this condition. On the other hand, it's easy to generate waves when the cylinder close to the free surface and wave will affect vortex shedding.

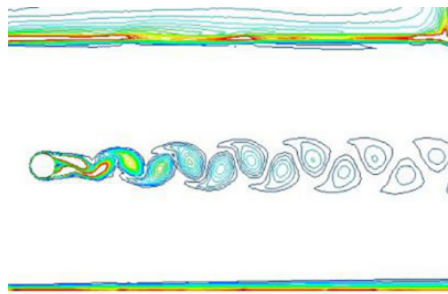


Figure 6(a). Vorticity magnitude of the cylinder for $H/D=5$

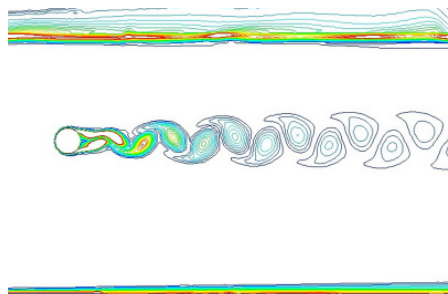


Figure 6(b). Vorticity magnitude of the cylinder for $H/D=4$



Figure 6(c). Vorticity magnitude of the cylinder for $H/D=3$

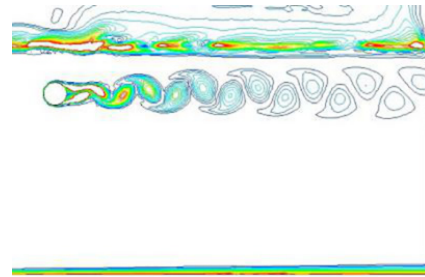


Figure 6(d). Vorticity magnitude of the cylinder for $H/D=2$

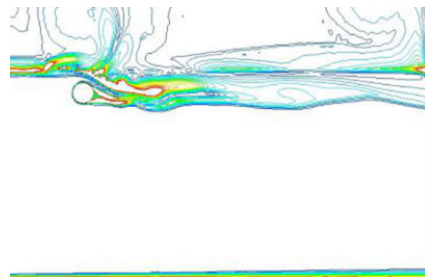


Figure 6(e). Vorticity magnitude of the cylinder for $H/D=1$

3.1.2 Effect of Reynolds Number

Figure 7 presents the vorticity magnitude at different Reynolds number for $H=4D$, to clarify the effect of Reynolds number on the vorticity magnitude. As the value of Reynolds number increasing, the size of vortices become more big and the number of vortices increase.

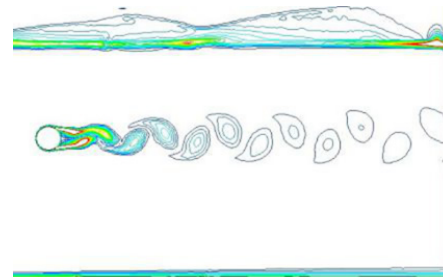


Figure 7(a). Vorticity magnitude of the cylinder for $Re=150624$

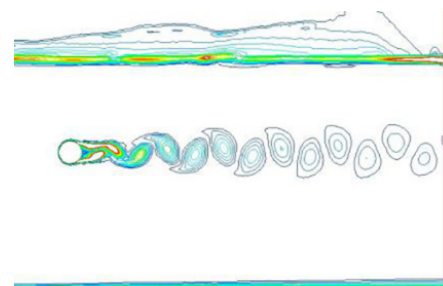


Figure 7(b). Vorticity magnitude of the cylinder for $Re=271123$

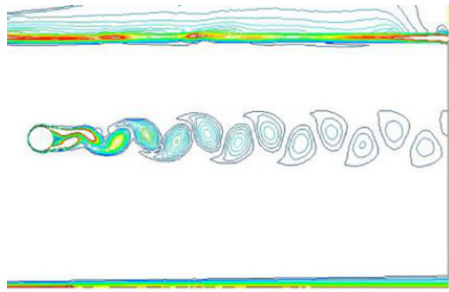


Figure 7(c). Vorticity magnitude of the cylinder for Re=210874

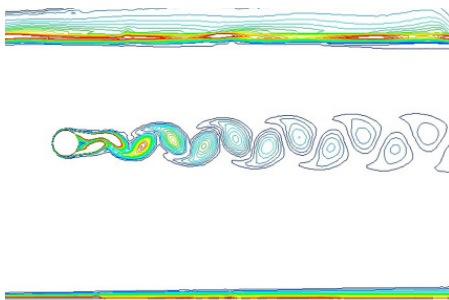


Figure 7(c). Vorticity magnitude of the cylinder for Re=331373

3.1.3 Results of Flow Parameters on the Cylinder

3.1.3.1 Drag Coefficients

The variation of the mean drag coefficient on the cylinder with submergence depth is present in Figure 8 for different Reynolds number.

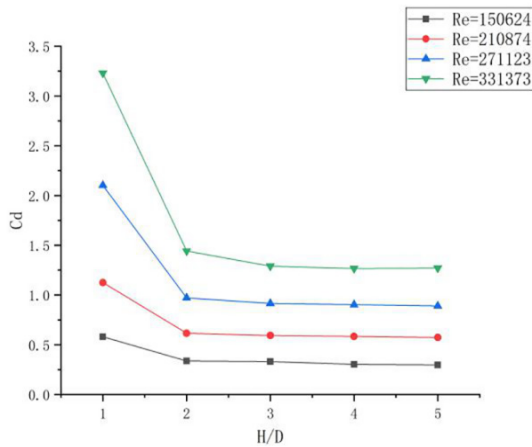


Figure 8. Variation of Cd of cylinder in different Reynolds number

As the H/D increases, the mean drag coefficient on the cylinder becomes smaller at all the Reynolds number. The value of Cd decreases more intense with higher Reynolds

number, especially when $H/D < 3$. Because when the cylinder close to the free surface, fluctuation and deformation of free surface will disturb the flow field around the cylinder, thus affect the drag force on the cylinder. When $H/D \geq 3$, as submergence depth increases, the influence of free surface becomes smaller.

The mean value of C_d increases as Reynolds number increases at all the submergence depth. C_d will increase sharply if the cylinder is very close to the free surface. As the H/D increase, the growth trend for C_d has slowed.

3.1.3.2 Lift Coefficients

The variation of the root square(RMS) value of lift coefficient on the cylinder with submergence depth is present in Figure 9 for different Reynolds number.

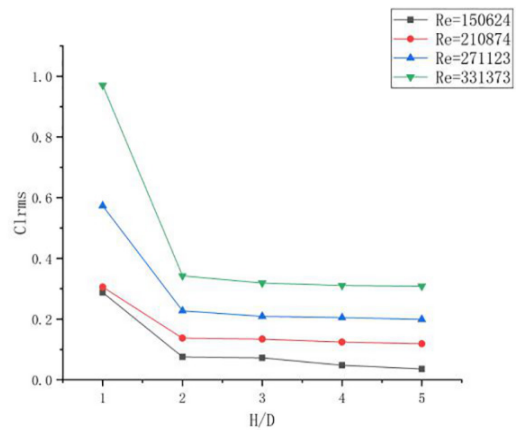


Figure 9. Variation of Cl_{rms} of cylinder in different Reynolds number

The RMS value of lift coefficient will decrease as H/D increase at all the Reynolds number. When $H/D < 2$, Cl_{rms} will decline acutely as H/D become bigger, when $H/D \geq 2$, the decline has moderated. Figure 10 clarify the dynamic pressure with different submergence depth for Re=331373. As figure.10(e) clarify, the free surface will have a remarkable influence on the formation of upper cylinder pressure field, thus affect the lift coefficient, even the position of the maximum pressure has changed due to the effect of free surface. Another reason why the free surface will influence lift coefficient, lift force is caused by the pressure increases on the surface of the cylinder when the vortex shed from one side of the cylinder, resulting in the pressure difference in the transverse direction of the cylinder. So lift coefficient will affect by H/D because the free surface will influence vortex shedding.

As Reynolds number increases, the RMS value of Cl increases at all the submergence depth,. Cl_{rms} will increase sharply if the cylinder is very close to the free surface. As the H/D increase, the growth trend becomes slow.

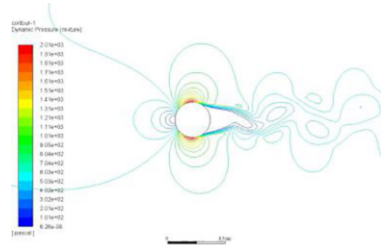


Figure 10(a). Pressure contour of the cylinder for H/D=5

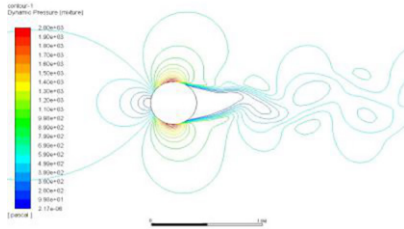


Figure 10(b). Pressure contour of the cylinder for H/D=4

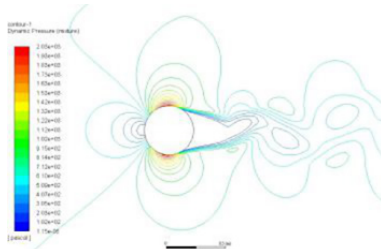


Figure 10(c). Pressure contour of the cylinder for H/D=3

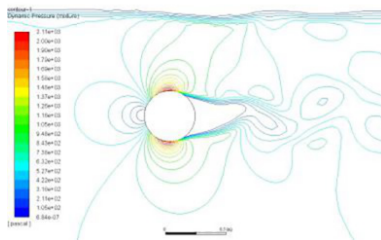


Figure 10(d). Pressure contour of the cylinder for H/D=2

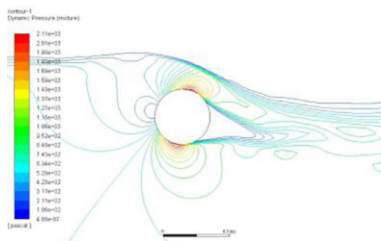


Figure 10(e). Pressure contour of the cylinder for H/D=1

3.1.3.3 Strouhal Number

The variation of St number on the cylinder with submergence depth is present in Figure 11 for different Reynolds numbers.

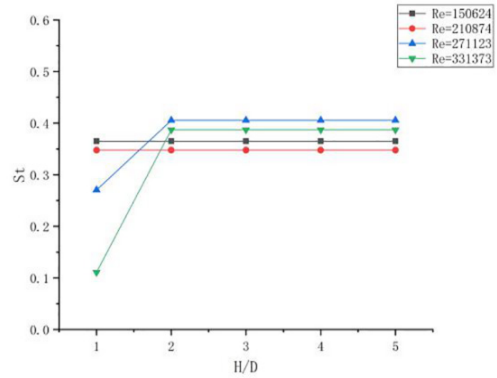


Figure 11. Variation of St of cylinder in different Reynolds number

Strouhal number will not change with submergence depth at $Re=150624$ and $Re=210874$. With $Re=271123$ and $Re=331373$, Strouhal number will increase first and flatten out when $H/D \geq 2$. Between $H/D=1$ and $H/D=2$, the higher Reynolds number is, the more drastic the change in Strouhal number. When $H/D < 2$, as the submergence depth increase, the boundary layer thickness on the upper surface of the cylinder increases, the negative and positive vortices shedding become more smoothly. Due to this reason, Strouhal number increases. As the submergence depth increases when $H/D \geq 2$, the thickness of the boundaries on the upper and down surface of the cylinder becomes approximately the same, so the Strouhal number will no longer affect by submergence depth. This effect is obvious when the Reynolds number is large.

3.2 Results of Cylinder with Addition Fairing

3.2.1 Effect of Submergence Depth

Figure 12 presents the vorticity magnitude at various submergence depth for $Re=331373$. With additional fairing, there is no vortex shedding in the wake, so when $H/D \geq 2$, the free surface will have little effect on wake. But wake will also damage by waves when the fairing is too close to the free surface.

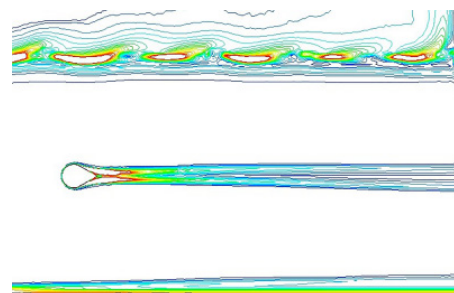


Figure 12(a). Vorticity magnitude of the cylinder with additional fairing for H/D=5

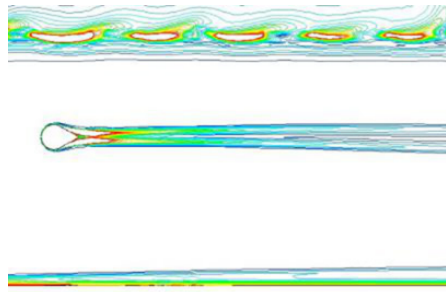


Figure 12(b). Vorticity magnitude of the cylinder with additional fairing for $H/D=4$

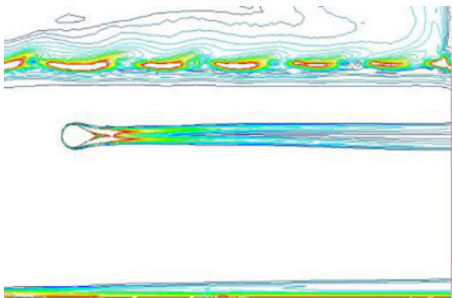


Figure 12(c). Vorticity magnitude of the cylinder with additional fairing for $H/D=3$

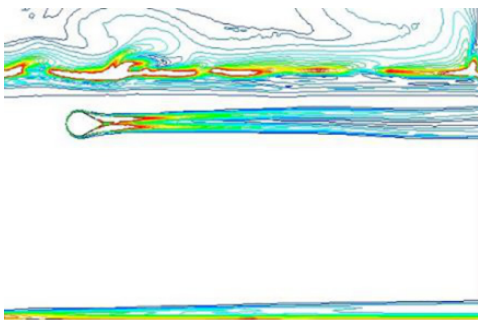


Figure 12(d). Vorticity magnitude of the cylinder with additional fairing for $H/D=2$

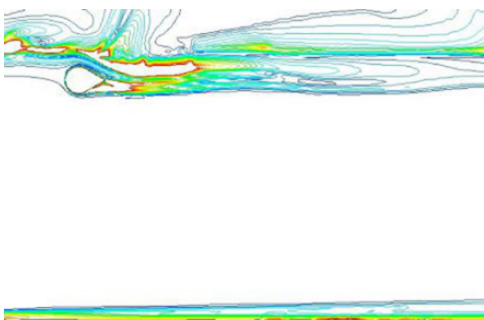


Figure 12(e). Vorticity magnitude of the cylinder with additional fairing for $H/D=1$

3.2.2 Effect of Reynolds Number

Figure 13 presents the vorticity magnitude at differ-

ent Reynolds number for $H=4D$, to clarify the effect of Reynolds number on the vorticity magnitude. When the Reynolds number is small, some small vortices can be observed in the wake. As the Reynolds number increases, the vortices gradually disappear.

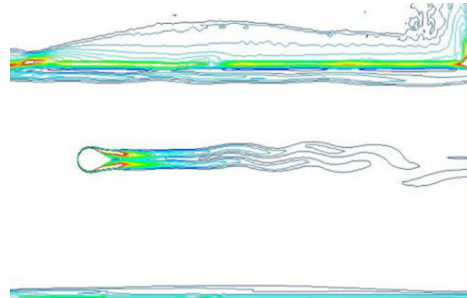


Figure 13(a). Vorticity magnitude of the cylinder for $Re=150624$

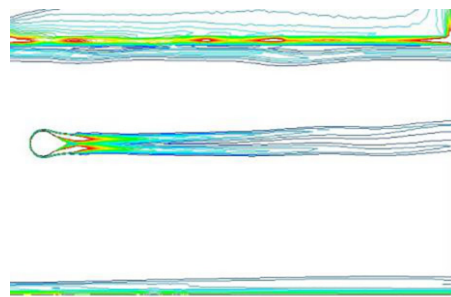


Figure 13(b). Vorticity magnitude of the cylinder for $Re=271123$

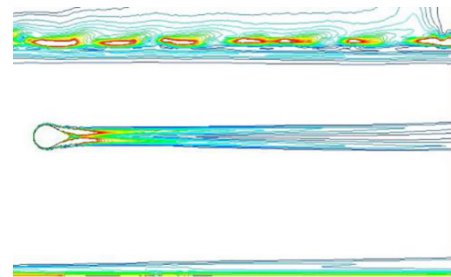


Figure 13(c). Vorticity magnitude of the cylinder for $Re=210874$

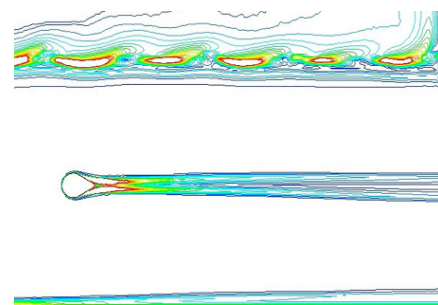


Figure 13(d). Vorticity magnitude of the cylinder for $Re=331373$

3.2.3 Results of Flow Parameters on the Cylinder

3.2.3.1 Drag Coefficients

The variation of the mean drag coefficient on the cylinder with additional fairing with submergence depth is present in Figure 14 for different Reynolds number.

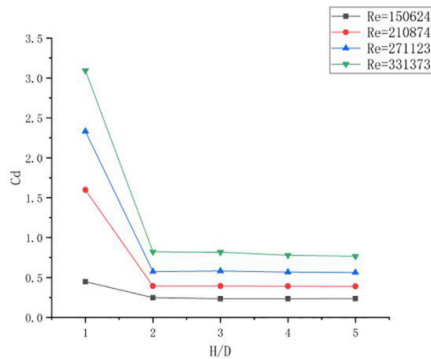


Figure 14. Variation of Cd of cylinder with additional fairing in different Reynolds number

When $H/D < 2$, as value of H/D increases, the C_d will decrease, when $H/D \geq 2$, C_d is hardly affected by the H/D value at all Reynolds number. Since there is no vortex shedding in the wake, the effect of the free liquid surface on the C_d value is reduced. However, when the fairing is too close to the free surface, the free surface is severely deformed due to the existence of the fairing, which affects the wake, and has a serious impact on the C_d value. Similar to the situation in the cylinder, the C_d will increase with the increase of the Reynolds number, but compare with Figure 8, the growth trend is obviously slower. It can be seen that fairing can reduce the influence of the free surface to a certain extent, especially when the Reynolds number is low.

3.2.3.2 Lift Coefficients

The variation of the RMS value of lift coefficient on the cylinder with additional fairing with submergence depth is present in Figure 15 for different Reynolds number.

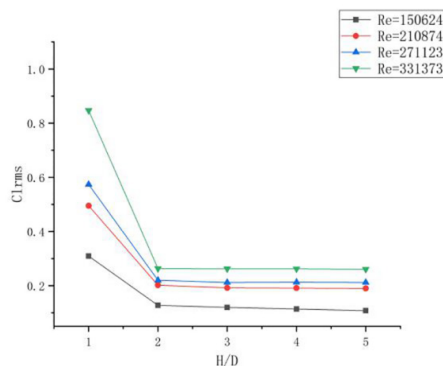


Figure 15. Variation of $C_{l_{rms}}$ of cylinder in different Reynolds number

When $H/D < 2$, $C_{l_{rms}}$ will decrease with H/D increases at all Reynolds number. When $H/D \geq 2$, C_l has a slight decrease when $Re=150624$ and $Re=21087$, remains stable at $Re=271123$ and $Re=331373$. At low Reynolds number, the free surface will promote the formation and shedding of vortices, so the $C_{l_{rms}}$ will decline when submergence depth increase. With big Reynolds numbers, since there are no vortex shedding in the wake, the submergence depth will have limited effect on $C_{l_{rms}}$. As Figure 16 clarify, although there is no effect of vortex shedding, the free surface still has a great influence on the pressure field above the fairing, which in turn affects the lift coefficient.

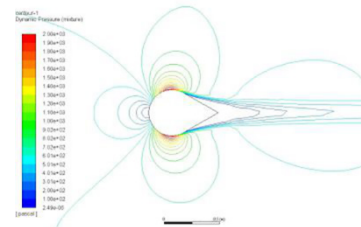


Figure 16(a). Pressure contour of the cylinder with additional fairing for $H/D=5$

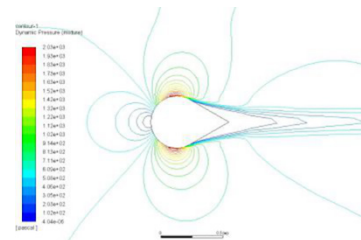


Figure 16(b). Pressure contour of the cylinder with additional fairing for $H/D=4$

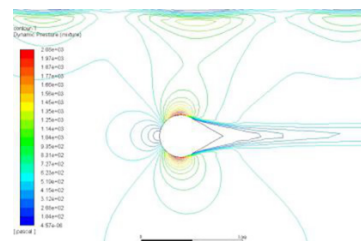


Figure 16(c). Pressure contour of the cylinder with additional fairing for $H/D=3$

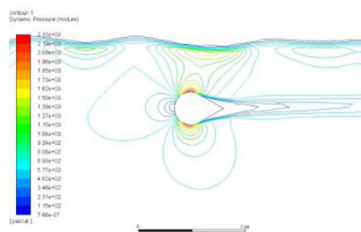


Figure 16(d). Pressure contour of the cylinder with additional fairing for $H/D=2$

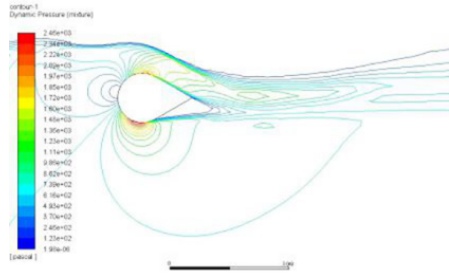


Figure 16(e). Pressure contour of the cylinder with additional fairing for $H/D=1$

3.2.3.3 Strouhal Number

The variation of St number on the cylinder with additional fairing with submergence depth is present in Figure 17 for different Reynolds number.

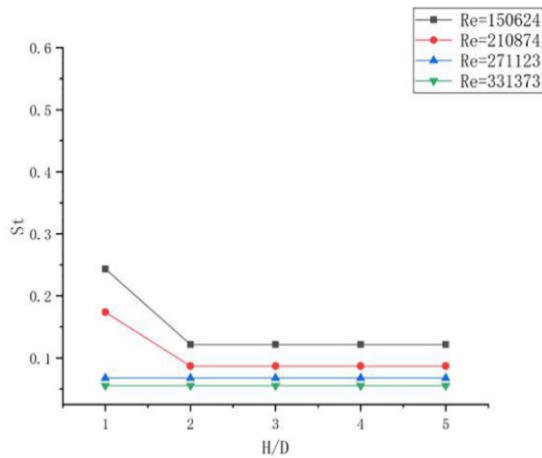


Figure 17. Variation of St of cylinder in different Reynolds number

When the fairing is close to the water surface, at low Reynolds number, the free surface will promote the formation and shedding of vortices, making Strouhal numbers increase. Therefore, for the low Reynolds number, H/D has a greater impact on Strouhal numbers. When $H/D < 2$, the Strouhal numbers will increase as H/D increase. When $H/D \geq 2$, as the submergence depth increases, the influence of the free surface decreases and the Strouhal numbers tend to stabilize. At a high Reynolds number, since there are no vortices, it has almost no effect on Strouhal numbers.

3.3 Comparison of the Results of the Two Structures

3.3.1 Drag Coefficient

The variation of the drag coefficient with submergence depth is present in Figure 18 for different structures.

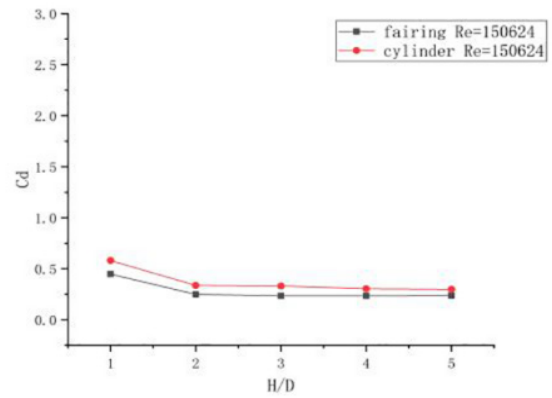


Figure 18(a). Variation of Cd of two different structure in $Re=150624$

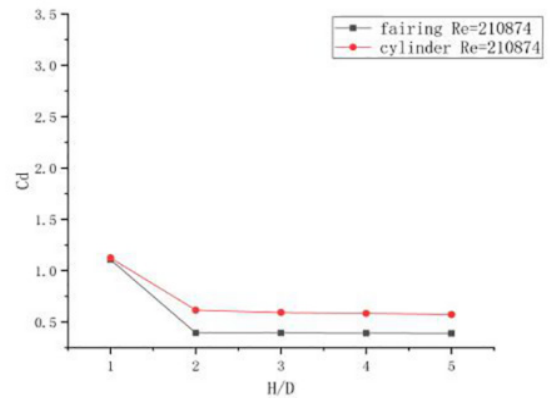


Figure 18(b). Variation of Cd of two different structure in $Re=271123$

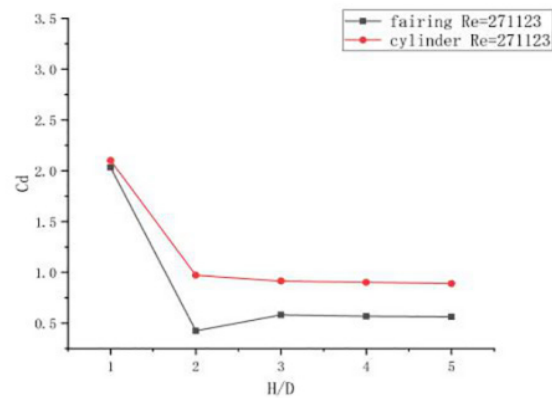


Figure 18(c). Variation of Cd of two different structure in $Re=210874$

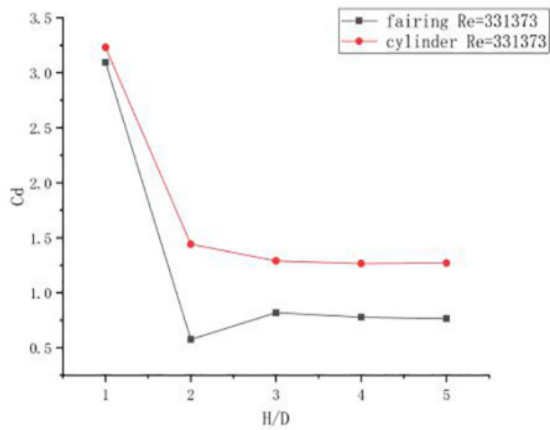


Figure 18(d). Variation of Cd of two different structure in Re=331373

The use of fairing can effectively reduce Cd, and the larger the Reynolds number, the more obvious the effect. The drag force is formed by the pressure difference between the front and back of the cylinder. The larger the Reynolds number, the greater the pressure difference and the greater the drag coefficient. The fairing can effectively reduce the pressure difference between the front and rear of the cylinder, thereby reducing the drag coefficient. But the structure has little effect on Cd when it's too close to the free surface, which is caused by the destruction of the free surface.

3.3.2 Lift Coefficient

The variation of the RMS lift coefficient with submergence depth is present in Figure 19 for different structures.

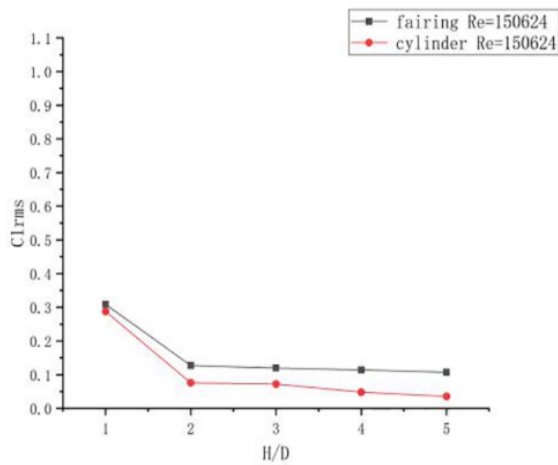


Figure 19(a). Variation of Cl_{rms} of two different structure in Re=150624

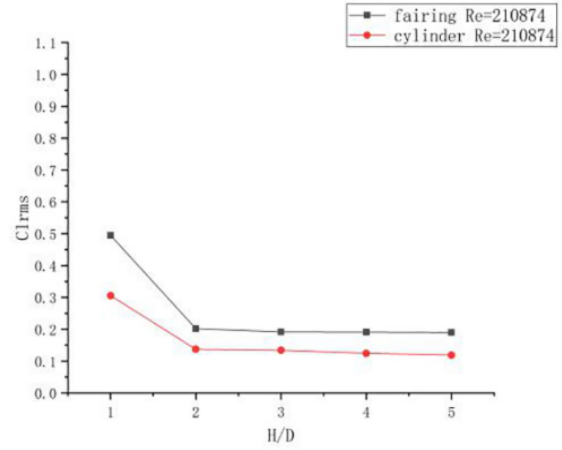


Figure 19(b). Variation of Cl_{rms} of two different structure in Re=271123

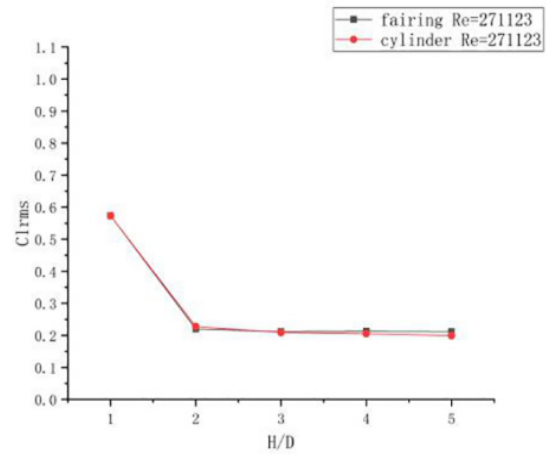


Figure 19(c). Variation of Cl_{rms} of two different structure in Re=210874

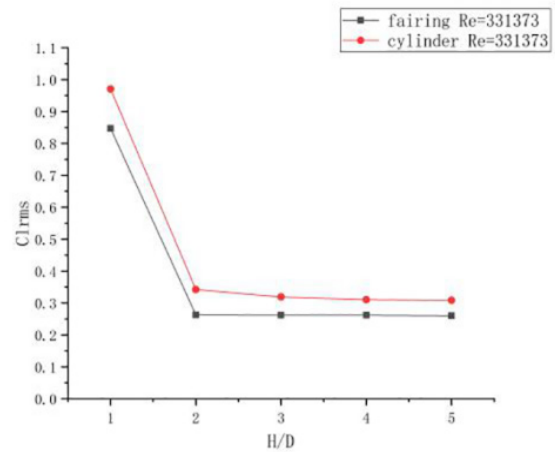


Figure 19(d). Variation of Cl_{rms} of two different structure in Re=331373

At low Reynolds number, the Cl_{rms} of the cylinder is smaller than that of the fairing. When the Reynolds number is low, there is still vortex shedding in the wake of the fairing, and the vortices in the wake are more big and further away from the center line compare with those in cylinder's wake, which cause bigger Cl_{rms} . As the Reynolds number increases, there is no vortex shedding in the wake of the fairing, Cl_{rms} will become smaller than the cylinder at all value of H/D .

3.3.3 Strouhal Number

The variation of the Strouhal number with submergence depth is present in Figure 20 for different structures.

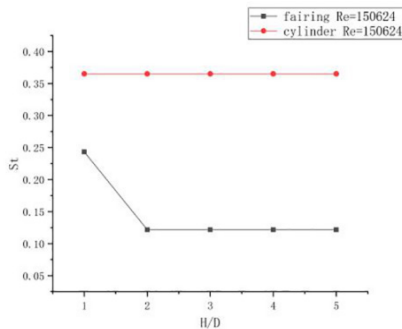


Figure 20(a). Variation of St of two different structure in $Re=150624$

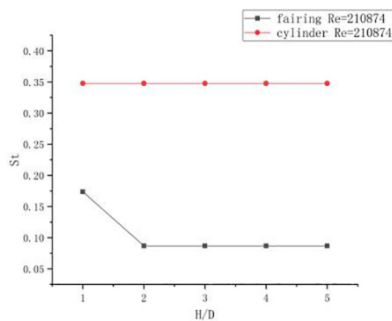


Figure 20(b). Variation of St of two different structure in $Re=271123$

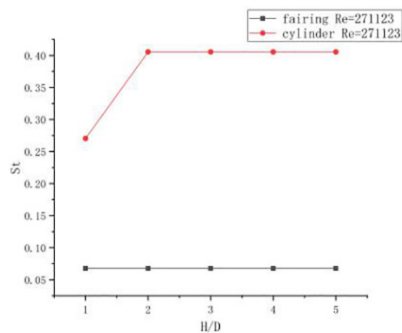


Figure 20(c). Variation of St of two different structure in $Re=210874$

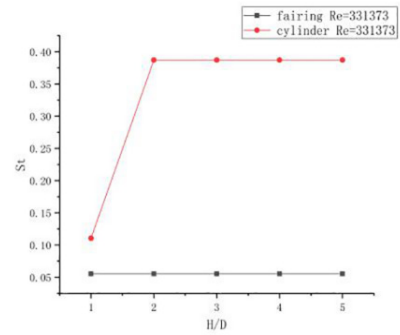


Figure 20(d). Variation of St of two different structure in $Re=331373$

When the Reynolds number is large, the St value is smaller for cylinder with additional fairing. It indicates that the frequency of vortex shedding is lower under this condition when the Reynolds number and characteristic length are the same. This is because the fairing suppresses the interaction of the shear layers on both sides to a certain extent, thereby suppressing the vortices that alternately shed off. It can be seen that the additional fairing can well suppress the vortex induced vibration. When the Reynolds number is small, part of the vortex remains detached from the wake, and the fairing will increase the St value, indicating that the frequency of vortex shedding is higher under this condition. In general, the value of H/D has little influence on St values of both structures, especially when $H/D \geq 2$.

In summary, the existence of the fairing can effectively reduce the Cd value, and effectively reduce the Cl_{rms} value and St value under high Reynolds number, but in the case of low Reynolds number, it will increase the Cl_{rms} value and St value. Therefore, the use of the fairing in the case of high Reynolds number can effectively reduce the drag force and effectively suppress the vortex-Induced vibration.

3. Conclusions

In this study, the flow around cylinder and cylinder with additional fairing placed in a free surface channel was investigated numerically. When the cylinder close to the free surface, the drag coefficient will increase, and the larger the Reynolds number, the more obvious this trend. After attaching the fairing, when $H/D \geq 2$, the free surface has a relatively small effect on the drag coefficient, and when the Reynolds number is high, the fairing has a significant effect on reducing the drag coefficient of the cylinder. The lift coefficient will also increase as the cylinder close to the free surface. In the case of high Reynolds number, the additional fairing can reduce the

lift coefficient, but in the case of low Reynolds number, it will increase the lift coefficient conversely. When the Reynolds number is low, H/D has no obvious effect on the Strouhal number of the cylinder, but under high Reynolds number, when $H/D < 2$, Strouhal number will increase as the increase of H/D , and the larger the Reynolds number, the increasing trend is more obvious. With the addition of the fairing, H/D has a small effect on Strouhal number under high Reynolds number, and has a greater effect under low Reynolds number. The fairing can reduce Strouhal number at all Reynolds number, which can effectively suppress vortex induced vibration. The main reason for these phenomena is that free surface breaks the vortex shedding, with additional fairing, there's less vortex shedding in wake, so the free surface will have influence on drag coefficient and Strouhal number. At low Reynolds number, due to the vortex in the wake, the lift coefficient of the fairing is larger than that of the cylinder. As the Reynolds number increases, the vortex disappears, and the lift coefficient of the fairing is gradually smaller than that of the cylinder.

Data Availability

The data that support the findings of this study are available from the corresponding author upon reasonable request.

References

- [1] Schewe G. On the force fluctuations acting on a circular cylinder in cross flow from subcritical up to transcritical Reynolds numbers. *J Fluid Mech* 1983;133.265–85.
- [2] Bearman, P. W. On vortex shedding from a circular cylinder in the critical Reynolds number regime. *Journal of Fluid Mechanics*, 1969,37(3), 577-585.
- [3] Breuer, Michael. A challenging test case for large eddy simulation: high Reynolds number circular cylinder flow. *International Journal of Heat and Fluid Flow*, 2000, 21.5: 648-654.
- [4] Yu D, Kareem A. Numerical simulation of flow around rectangular prism[J]. *Journal of wind engineering and industrial aerodynamics*, 1997, 67: 195-208.
- [5] Suh J, Yang J, Stern F. The effect of air water interface on the vortex shedding from a vertical circular cylinder. *ASME J Fluids Eng* 2011; 27:1-22.
- [6] Graf, W. H., & Yulistiyanto, B. Experiments on flow around a cylinder; the velocity and vorticity fields. *Journal of Hydraulic Research*, 1998,36(4), 637-654.
- [7] Kawamura, T., et al. "Large eddy simulation of a flow past a free surface piercing circular cylinder." *Transactions-American Society of Mechanical Engineers Journal of Fluids Engineering*.124.1 (2002): 91-101.
- [8] Wu, C.J., Wang, L., Wu, J.Z. Suppression of the von Kármán vortex street behind a circular cylinder by a travelling wave generated by a flexible surface. *Journal of Fluid Mechanics*, 2007, 574, 365-391.
- [9] Kim J, Choi H. Distributed Forcing of Flow over a Circular Cylinder[J]. *Physics of Fluids*, 2005, 17: 033103 1-16.
- [10] Wu Yucheng, Wu Shiyuan. ADINA-FSI analysis of vortex induced suppression effect of spiral strake and fairing[J]. *China Petroleum and Chemical Standards and Quality*, 2013,07:65.